Science and Technology Indonesia
e-ISSN:2580-4391 *p*-ISSN:2580-4405
Vol. 8, No. 4, October 2023

Research Paper

In Silico Analysis of Phenolic Compounds from *Ceriops decandra* Griff. Leaves and Molecular Interaction as Anti Diabetes

Yunita Eka Puspitasari[1], Mochamad Arega Alfikri [1], Romasni Sitanggang [1], Jeny Ernawati Tambunan [1], Hardoko Hardoko[1*]

[1]*Department of Fish Product Technology, Faculty of Fisheries and Marine Sciences Universitas Brawijaya, Jl. Veteran Malang, 65145, Indonesia*
***Corresponding author**: hardoko@ub.ac.id*

Abstract
α-amylase and α-glucosidase in the gastrointestinal tract have an important role in the hydrolysis α-1,4 and α-1,6 glycosidic chain of starch, respectively. Inhibition of both enzyme activities becomes one of the strategies to control diabetes. However, commercial drugs such as antidiabetics have adverse effects such as gastrointestinal problems. Therefore, exploring functional food, especially from marine natural products as antidiabetic agents, is potential. In particular, *Ceriops sp*. was reported to contain bioactive compounds with antidiabetic properties, but its mechanism to treat diabetes has not been proved. The potency of phenolic compounds of *C. decandra* leaves as α-amylase and α-glucosidase inhibitors were examined in this research by implementing the molecular docking analysis in silico. Three steps of analysis were carried out in this study, including extraction from *C. decandra* leaves with different polarity solvents, identification of phenolic compounds using LC-HRMS, and molecular docking analysis of phenolic compounds identified from *C. decandra* leaves. This study revealed that quercetin, rutin, epicatechin, isorhamnetin, caffeic acid, and ferulic acid were identified from *C. decandra* leaves. According to the drug-likeness and toxicity analysis, the presented compounds in *C. decandra* leaves had high potential pharmacological properties. Furthermore, molecular interaction analysis exhibited phenolic compounds extracted with ethyl acetate, such as quercetin and epicatechin, and with methanolic extracts, such as quercetin, rutin, epicatechin, and isorhamnetin, were more effective as α-amylase and α-glucosidase inhibitors than from caffeic acid and ferulic acid. Among the phenolic compounds of *C. decandra* leaves, rutin and quercetin were predicted to be the potential α-glucosidase inhibitors.

Keywords
Ceriops sp., in Silico, α-amylase, Flavonoid, Phenolic Compound, α-Glucosidase

Received: 10 February 2023, Accepted: 7 May 2023
https://doi.org/10.26554/sti.2023.8.4.542-553

1. INTRODUCTION

Diabetes mellitus (DM) is defined as a metabolic disorder characterized by an increase in blood glucose due to a decrease in insulin secretion. This condition leads to metabolism disorders of lipids, proteins and carbohydrates (Hossain et al., 2016). In terms of the incidence, the number of diabetes in adults were predicted to increase to 500 million in 2035, especially in South-East Asia, reaching 123 million. Two common types of diabetes include type 1 and type 2. In a prior study, it was reported that more than 90% of patients suffered from T2DM (Kharroubi and Darwish, 2015).

Digestion of dietary carbohydrates involves two enzymes, such as: (1) pancreatic α-amylase hydrolyze of α-1, 4 glycosidic linkages in polysaccharides to produce maltose, maltotriose, and α-dextrins; and (2) α-glucosidase hydrolyze α-1,6 glycosidic linkages to produce glucose. Further, glucose is transported into cells via sodium-dependent glucose transporter (SGLT1) located in the brush border of the intestine (Kim et al., 2016). T2DM management is performed to delay glucose absorption through the inhibition of both inhibitors (α-glucosidase and α-amylase) in the digestive organs (Riyaphan et al., 2021). Another study reported that both α-glucosidase and α-amylase inhibitors significantly reduce blood glucose levels and; therefore, the inhibitors can be consumed by T2DM patients to control postprandial hyperglycemia (Chen and Kang, 2013; Udrea et al., 2021). One of the pharmacological approaches to treat diabetes includes a series of antidiabetic drugs, such as sulfonylureas, biguanide, thiazolidinedione, and α-glucosidase inhibitors. In particular, α-glucosidase inhibitors such as acarbose, miglitol, and voglibose proved to be the most effective agents in decreasing blood glucose levels in T2DM (Derosa and Maffioli, 2012). However, commercial drugs present adverse effects, mainly related to gastrointestinal problems such as flatulence, abdominal distention, and diarrhea (Chen and Kang, 2013; Derosa and Maffioli, 2012). Consequently, in order to cope with the side effect of commercial

drugs, diabetic patients consume both conventional medicine and food supplement to maintain the fluctuations of blood glucose levels and to complement diabetes treatment (Dham, 2006; Zhang et al., 2017). Thus, the exploration of food supplements, especially from marine resources, has attracted society and researchers (Lauritano and Ianora, 2016).

As presented in this study, the marine resources include mangrove plants which grow along the tropical and sub-tropical coastline in high salinity areas. Typically, mangroves have been utilized in traditional medicine and claimed to contain biological activities such as antioxidant, antimicrobial, and antidiabetic. The prominent secondary metabolite in the mangrove plant is tannin (Bibi et al., 2019). In particular, mangrove plant such as *Rhizophora sp*. presents a good source of tannin and flavonoid, implemented as an antidiabetic agent in South East Asia (Hardoko et al., 2015; Hardoko et al., 2017; Lawag et al., 2012; Hardoko et al., 2016; Trinh et al., 2016). Ceriops becomes one of the mangrove plants consisting of five species, such as *C. tagal*, *C. decandra*, *C. pseudodecandra*, *C. zippeliana* and *C. australis*. Specifically, *C. tagal* leaves are extracted by employing different solvents such as methanol, ethanol, ethyl acetate, and petroleum ether, inhibiting α-glucosidase and α-amylase activity. In further process, a prior study reported that the phytochemical screening of *C. tagal* leaves depicts alkaloid, tannin, terpenoid, glycoside, steroid, saponin, flavonoid, anthocyanin, coumarin, phenolic, and quinone (Jadhav, 2019). Bioactive compounds isolated from *C. tagal* were dominated by terpenoid lupeol, betulin, and belong (Ramadhan et al., 2020). Commonly, *Ceriops sp*. has been consumed as a traditional food by the mangrove society in Indonesia (Askama et al., 2017; Mahmud, 2011; Prabowo, 2018). Meanwhile, *C. decandra* is one of the mangrove plants growing in Indonesia (Alamsjah and FauzulImron, 2021), and potentially used as a traditional medicine to treat diabetes (Lawag et al., 2012), containing oleanolic acid, exhibiting an anti-inflammatory agent. The leaves of *C. decandra* also contain catechin, which is consumed to prevent cancer in humans (Mahmud et al., 2018). However, the exploration of phytochemical compounds in *C. decandra* as antidiabetic agent is limited. Even though catechin was identified from their leaves, other flavonoid, and phenolic compounds have not been reported yet. The mechanism of phytochemical compounds extracted from *C. decandra* leaves as an antidiabetic agent has not been determined. Referring to such findings, this study aimed to investigate the potency of phenolic compounds of *C. decandra* leaves as α-amylase inhibitor by using *in silico* molecular docking method.

2. EXPERIMENTAL SECTION

2.1 Materials

Fresh *C. decandra* leaves of the second, third, and fourth shoots were harvested from Clungup Mangrove Conservation, Malang, Indonesia. The obtained plant material was identified at Materia Medika, Batu, Indonesia (No. 074/129/102.20-A/2022). Three different solvents (pa), including n-hexane, ethyl-acetate, and methanol from Smart-Lab, Tangerang, Indonesia, were used in this investigation.

2.2 Method

2.2.1 Preparation of *C. decandra* Leaves Extract

The air-dried and powdered plant was extracted for 3x24 hr, with different polarity solvents, including n-hexane, ethyl acetate, and methanol, respectively. Initially, the powdered leaves (15 g) were defatted with n-hexane (3x225 mL). The residue was macerated with ethyl-acetate (3x225 mL) and the polar solvent, methanol (3x225 mL) was added to the residue of ethyl acetate. The ethyl acetate and methanol filtrate were concentrated by using a vacuum concentrator to obtain ethyl acetate extract (2.6 g) and methanol extract (7.0 g), respectively, and all extracts were kept at 4°C.

2.2.2 LC-HRMS Analysis

The present compounds in ethyl acetate and methanolic extract were identified by performing LC-HRMS analysis. However, *n*-hexane extract was not analyzed because the compound tends to be a lipophilic compound, which was excluded in this study. LC-HRMS analysis was performed by HPLC-Thermo Scientific Dionex Ultimate 3000 RSLCnano with a micro flow meter. The mobile phase consisted of A: Water+0.1% formic acid and B: acetonitrile+0.1% formic acid. The separation was performed on Column Hypersil Gold aQ with 50 x 1 mm x 1.9 μ particle size. The flow rate was sustained in 40 μL/min. The mass spectrometer Thermo Scientific Q Exactive was run in positive ion mode for 30 minutes with a full scan resolution of 70,000.

2.2.3 Drug-likeness and Toxicity Analysis

The pharmacological properties of phenolic compounds extracted from *C. decandra* leave, including Lipinski's rule, were determined according to the SwissADME database http://www.\swissadme.ch/index.php. In addition, the Protox tool https://\tox-new.charite.de/protox_II/ was employed to predict the toxicity level and LD_{50}.

2.3 Molecular Interaction Analysis

2.3.1 Ligand Preparation

The phenolic compounds of *C. decandra* leaves, such as epicatechin, quercetin, rutin, isorhamnetin, ferulic acid, and caffeic acid, were identified by performing LC-HRMS analysis. The 3D ligand's structures were downloaded from the PubChem database https://pubchem.ncbi.nlm.nih.gov in SDF format. Native ligands such as NAG and MYC were retrieved (SDF format) from Protein Data Bank https://www.rcsb.org/. Additionally, the structure of acarbose, miglitol, and voglibose, as ligand control, were retrieved from PubChem database https://pubchem.ncbi.nlm.nih.gov in SDF format.

2.3.2 Protein Preparation

The crystal structure of α-amylase was retrieved from Protein Data Bank (PDB ID: 4GQR) https://www.rcsb.org/

Table 1. Phenolic Compound Identified from Ethyl Acetate *C. decandra* Leaves Extract

RT (min)	Calc. MW	Formula	Compound
0.868	302.04234	$C_{15}H_{10}O_7$	Quercetin
5.585	290.07881	$C_{15}H_{14}O_6$	Epicatechin
20.384	180.02415	$C_9H_8O_4$	Caffeic acid
22.141	194.05783	$C_{10}H_{10}O_4$	Ferulic acid

Table 2. Phenolic Compound Identified from Methanolic *C. decandra* Leaves Extract

RT (min)	Calc. MW	Formula	Compound
3.673	302.04234	$C_{15}H_{10}O_7$	Quercetin
3.675	610.15373	$C_{27}H_{30}O_{16}$	Rutin
3.685	290.07881	$C_{15}H_{14}O_6$	Epicatechin
8.146	316.05828	$C_{16}H_{12}O_7$	Isorhamnetin

with PDB ID: 4GQR and PDB ID: 3A4A, respectively. Furthermore, the protein receptor was prepared by removing the ligands and water molecules and by adding polar hydrogen to the protein through Biovia Discovery Studio 2019.

2.3.3 Chemical Interaction and Analysis

Molecular docking analysis was conducted by AutoDock Vina in PyRx software Trott and Olson (2010) to determine chemical interaction and binding energy among the selected compounds or ligands and α-amylase as a macromolecule. Furthermore, Open Babel was used to minimize the energy of the ligand and to convert the SDF format of ligands into PDBQT format. In molecular docking method, the grid box dimensions of protein α-amylase (PDB ID: 4GQR) were defined as center x= 8.4474, y= 27.9862, z= 49.1350 and dimensions x= 58.9736, y= 73.7796, and z= 58.5527. The grid box of receptor α-glucosidase was set as follows: $center_x$= 21.2711, $center_y$= -0.7586, $center_z$=18.6326; dimension x=56.7368, y=75.1330, z=65.4370. The ligands-enzyme interactions were saved in PDB format. Biovia Discovery Studio 2019 was implemented for graphical visualization of molecular interactions to analyze the hydrogen bond interaction and producing to produce the 3D and 2D images. The best interactions, indicated by protein and ligand, were determined based on the least binding energy (kcal/mol) (Sivakumar et al., 2021).

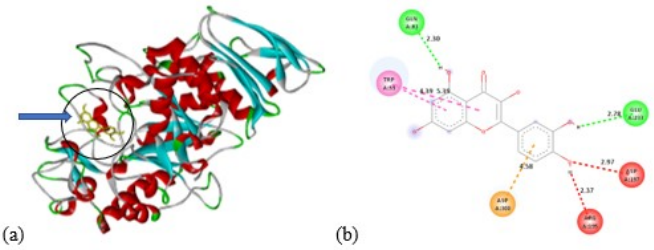

Figure 1. Visualization of 3D and 2D Molecular Interaction (a) and (b) Between α-amylase and Quercetin

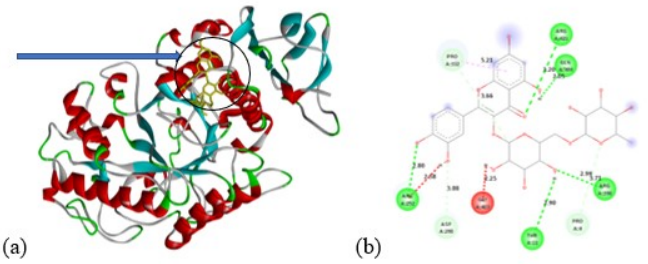

Figure 2. Visualization of 3D and 2D Molecular Interaction (a) and (b) Between α-amylase and Rutin

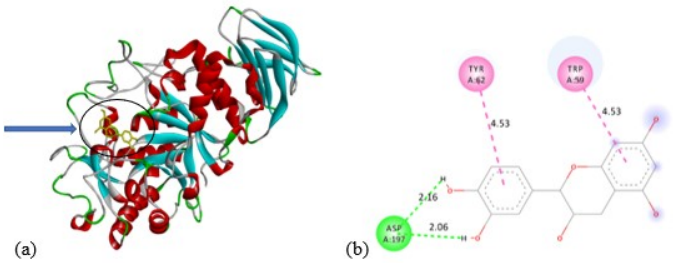

Figure 3. Visualization of 3D and 2D Molecular Interaction (a) and (b) Between α-amylase and Epicatechin

3. RESULTS AND DISCUSSION

3.1 Identification of Phenolic Compounds from *C. decandra* Leaves

Chemical constituents of *C. decandra* leaves were identified by LC-HRMS. In this experiment, the present authors detected the six flavonoid compounds from both ethyl acetate and methanol extract of *C. decandra* leaves. In particular, ethyl acetate extract of *C. decandra* leaves contained quercetin, epicatechin, caffeic acid, and ferulic acid (Table 1). Whereas methanol extract of *C. decandra* leaves contained quercetin, rutin, epicatechin, and isorhamnetin (Table 2). Quercetin and

Table 3. Druglikeness and Toxicity Analysis

Compound	Lipinski's Rule	Swiss ADME		Toxicity	
		Bioavailability	Gastrointestinal Absorption	LD_{50} (mg/kg)	Level
Quercetin	Yes	0.55	High	159	3
Rutin	No	0.17	High	5,000	5
Epicatechin	Yes	0.55	High	10,000	6
Isorhamnetin	Yes	0.55	Low	5,000	5
Caffeic acid	Yes	0.56	High	1,190	4
Ferrulic acid	Yes	0.85	High	1,772	4

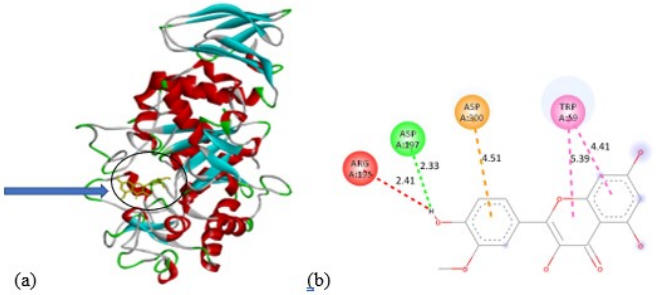

Figure 4. Visualization of 3D and 2D Molecular Interaction (a) and (b) Between α-amylase and Isorhamnetin

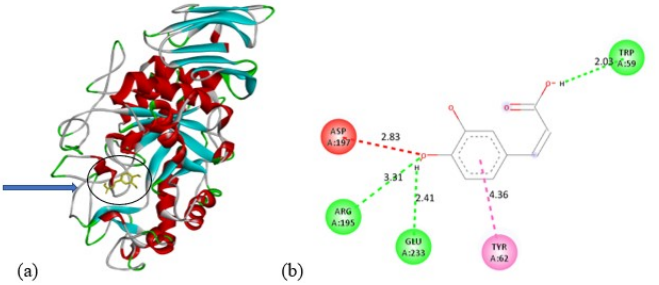

Figure 5. Visualization of 3D and 2D Molecular Interaction (a) and (b) Between α-amylase and Caffeic Acid

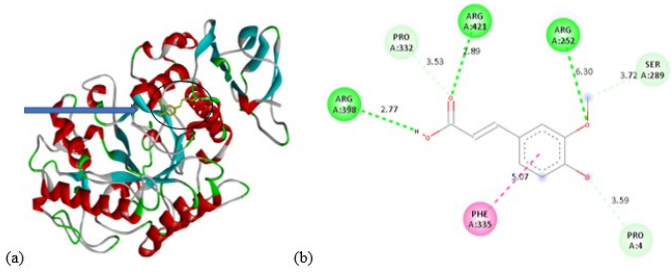

Figure 6. Visualization of 3D and 2D Molecular Interaction (a) and (b) Between α-amylase and Ferulic Acid

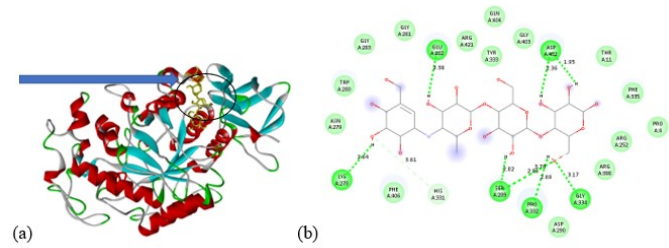

Figure 7. Visualization of 3D and 2D Molecular Interaction (a) and (b) Between α-amylase and Acarbose

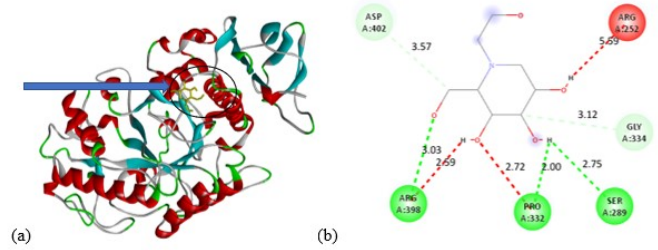

Figure 8. Visualization of 3D and 2D Molecular Interaction (a) and (b) Between α-amylase and Miglitol

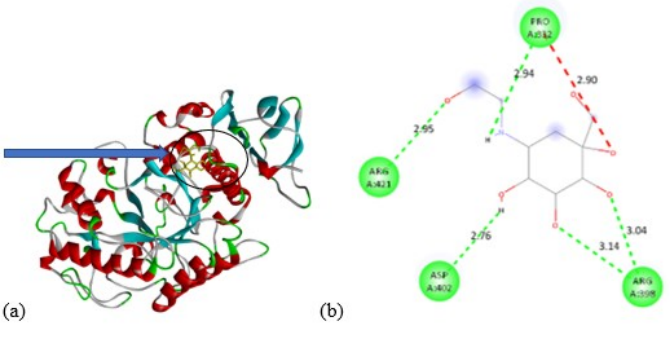

Figure 9. Visualization of 3D and 2D Molecular Interaction (a) and (b) Between α-amylase and Voglibose

Table 4. Molecular Interaction and Binding Energy of Phenolic Compounds Extracted from *C. decandra* Leaves with α-Amylase

Compound	Hydrogen Bond	Electrostatic	Hydrophobic Bond	Distance (Å)	Binding Energy (kcal/mol)
Quercetin	N:UNK1:H - A:GLU233:OE1			2.77559	-8.2
	N:UNK1:H - A:GLN63:OE1			2.30449	
		A:ASP300:OD2 - N:UNK1		4.58028	
			A:TRP59 - N:UNK1	5.39389	
			A:TRP59 - N:UNK1	3.9432	
			A:TRP59 - N:UNK1	4.40808	
Rutin	A:ARG252:NH2 - N:UNK1:O			2.80286	-8.7
	A:ARG398:NE - N:UNK1:O			2.9869	
	A:ARG421:NH2 - N:UNK1:O			3.20045	
	N:UNK1:H - A:GLN404:O			2.04929	
	N:UNK1:H - N:UNK1:O			2.0595	
	N:UNK1:H - N:UNK1:O			2.48039	
	N:UNK1:H - A:THR11:O			2.90135	
	A:PRO4:CD - N:UNK1:O			3.71336	
	A:ASP290:CA - N:UNK1:O			3.08419	
	N:UNK1:C - A:PRO332:O			3.66462	
			N:UNK1 - A:PRO332	5.2052	
Epicatechin	N:UNK1:H -A:ASP197:OD1			2.06398	-8.6
	N:UNK1:H - A:ASP197:OD1			2.15892	
			A:TRP59 - N:UNK1	4.14012	
			A:TRP59 - N:UNK1	3.9622	
			A:TYR62 - N:UNK1	4.52603	
Isorhamnetin	N:UNK1:H - A:ASP197:OD1			2.33248	-8.3
		A:ASP300:OD2 - N:UNK1		4.51209	
			A:TRP59 - N:UNK1	5.38608	
			A:TRP59 - N:UNK1	3.94888	
			A:TRP59 - N:UNK1	4.40001	
Caffeic acid	A:ARG195:NH2 - N:UNK1:O			3.31006	-6.5
	N:UNK1:H - A:TRP59:O			2.02606	
	N:UNK1:H - A:GLU233:OE2			2.40534	
			A:TYR62 - N:UNK1	4.35622	
Ferulic acid	A:ARG252:NH1 - N:UNK1:O			3.16097	-6.5
	A:ARG252:NH2 - N:UNK1:O			3.03187	
	A:ARG421:NH1 - N:UNK1:O			2.88786	
	N:UNK1:H - A:ARG398:O			2.76519	
	A:PRO4:CD - N:UNK1:O			3.58638	
	A:PRO332:CA - N:UNK1:O			3.52842	
	N:UNK1:C - A:SER289:O			3.72103	
			A:PHE335 - N:UNK1	5.07215	
Acarbose (control ligand)	A:SER289:OG - N:UNK1:O			2.85444	-8.1
	A:GLY334:N - N:UNK1:O			3.17498	
	N:UNK1:H - A:LYS278:O			2.63882	
	N:UNK1:H - A:GLU282:OE2			2.37909	
	N:UNK1:H - A:SER289:OG			2.82032	
	N:UNK1:H - N:UNK1:O			1.84647	
	N:UNK1:H - A:ASP402:OD1			2.35734	
	N:UNK1:H - A:ASP402:OD1			1.95064	
	N:UNK1:H - A:PRO332:O			2.6861	
	N:UNK1:H - N:UNK1:O			2.43991	
	A:HIS331:CE1 - N:UNK1:O			3.60577	
	N:UNK1:C - A:SER289:O			3.70476	
Miglitol (control ligand)	A:ARG398:NE - N:UNK1:O			3.02654	-5.3
	N:UNK1:H - A:SER289:OG			2.74774	
	N:UNK1:H - A:PRO332:O			1.99936	
	N:UNK1:C - A:GLY334:O			3.11626	
	N:UNK1:C - A:ASP402:OD1			3.57321	
Voglibose (control ligand)	A:ARG398:NE - N:UNK1:O			3.13884	-6.4
	A:ARG398:NH2 - N:UNK1:O			3.0416	
	A:ARG421:NH2 - N:UNK1:O			2.94614	
	N:UNK1:H - A:PRO332:O			2.936	
	N:UNK1:H - N:UNK1:O			2.53573	
	N:UNK1:H - A:ASP402:OD1			2.76368	

NAG (native ligand)	N:UNK1:H - A:GLU233:OE1		2.41992	-5.7
MYC (native ligand)	A:SER3:OG - N:UNK1:O		2.88539	-8.0
	A:THR6:OG1 - N:UNK1:O		2.70257	
	A:ARG398:NH2 - N:UNK1:O		3.28698	
	N:UNK1:H - A:ASP402:OD1		2.84976	
	N:UNK1:H - A:PRO332:O		2.67776	
	N:UNK1:H - A:GLY334:O		2.51017	
	N:UNK1:H - A:THR6:O		2.50085	
		N:UNK1 - A:PRO4	4.60738	
		N:UNK1 - A:PRO4	4.00008	

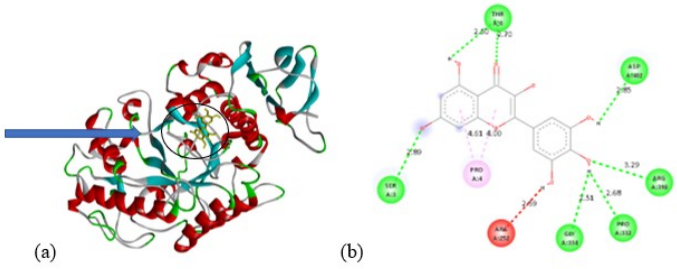

Figure 10. Visualization of 3D and 2D Molecular Interaction (a) and (b) Between α-amylase and Myricetin

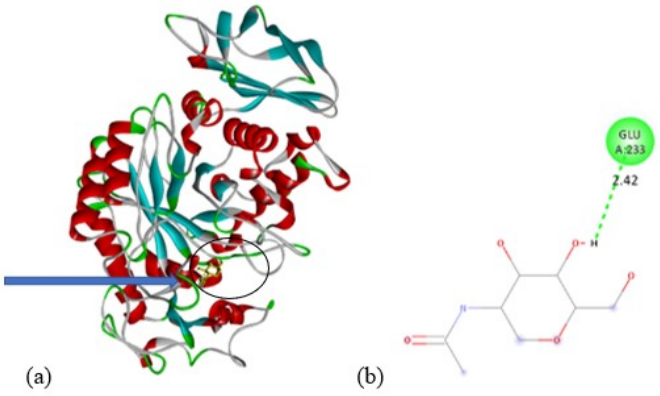

Figure 11. Visualization of 3D and 2D Molecular Interaction (a) and (b) Between α-amylase and Native Ligand 2 Acetamido 2 Deoxy Beta D Glucopyranose (NAG)

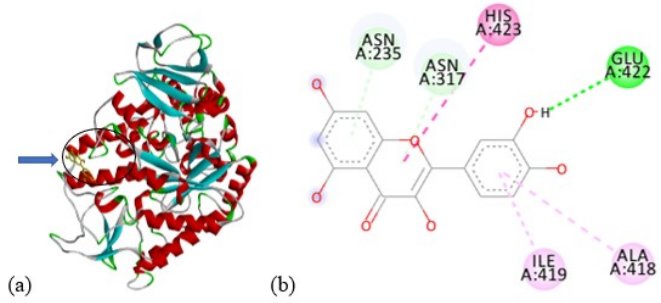

Figure 12. Visualization of 3D and 2D Molecular Interaction (a) and (b) Between α-glucosidase and Quercetin

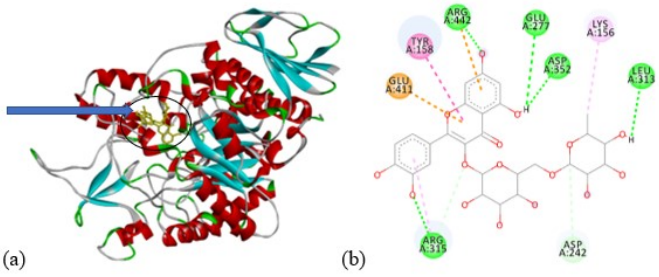

Figure 13. Visualization of 3D and 2D Molecular Interaction (a) and (b) Between α-glucosidase and Rutin

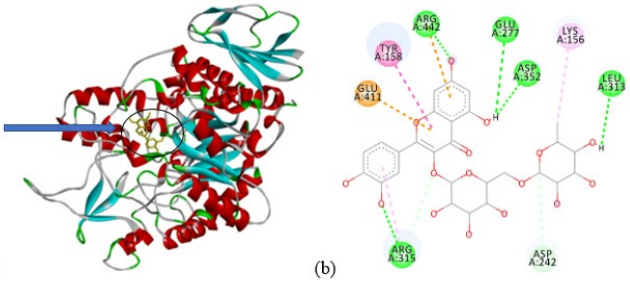

Figure 14. Visualization of 3D and 2D Molecular Interaction (a) and (b) Between α-glucosidase and Epicatechin

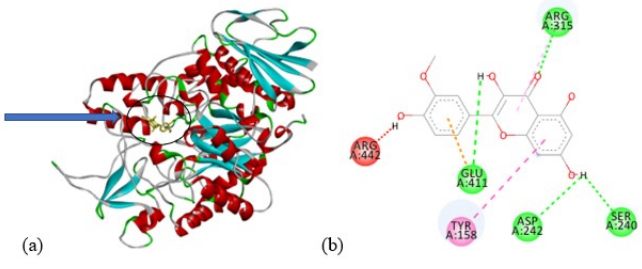

Figure 15. Visualization of 3D and 2D Molecular Interaction (a) and (b) Between α-glucosidase and Isorhamnetin

Table 5. Molecular Interaction and Binding Energy of Flavonoid Compounds Extracted from *C. decandra* Leaves with α-Glucosidase

Compound	Hydrogen Bond	Electrostatic	Hydrophobic Bond	Distance (Å)	Binding Energy (kcal/mol)
Quercetin	N:UNK1:H - A:GLU422:OE1			2.58907	-8.7
	N:UNK1:H - N:UNK1:O			2.56823	
	A:ASN235:HD21 - N:UNK1			2.55171	
	A:ASN317:HD22 - N:UNK1			3.02129	
			A:HIS423 - N:UNK1	5.29361	
			N:UNK1 - A:ALA418	5.41696	
			N:UNK1 - A:ILE419	4.99911	
Rutin	A:ARG315:HN - N:UNK1:O			2.68632	-10.5
	A:ARG442:HH12 - N:UNK1:O			2.44325	
	N:UNK1:H - A:GLU277:OE2			3.06396	
	N:UNK1:H - A:ASP352:OD2			2.46695	
	N:UNK1:H - A:LEU313:O			2.85898	
	A:ARG315:CD - N:UNK1:O			3.33397	
	N:UNK1:C - A:ASP242:OD2			3.16968	
		A:ARG442:NH1 -N:UNK1		3.75923	
		A:GLU411:OE2 -N:UNK1		4.02746	
			A:TYR158 - N:UNK1	5.38274	
			N:UNK1:C - A:LYS156	3.96234	
			N:UNK1 - A:ARG315	4.94513	
Epicatechin	N:UNK1:H - A:GLU411:OE2			2.22947	-8.4
	A:ARG315:CD - N:UNK1:O			3.43905	
			N:UNK1 - A:ARG315	4.51097	
Isorhamnetin	A:ARG315:HN - N:UNK1:O			2.25845	-8.4
	N:UNK1:H - A:GLU411:OE2			2.81979	
	N:UNK1:H - N:UNK1:O			2.34446	
	N:UNK1:H - A:SER240:OG			2.30316	
	N:UNK1:H - A:ASP242:OD1			3.06574	
		A:GLU411:OE2 - N:UNK1		3.37079	
			A:TYR158 - N:UNK1	5.51825	
			N:UNK1 - A:ARG315	4.96786	
Ferrulic acid	A:ARG315:HN - N:UNK1:O			2.25845	-6.9
	A:GLY161:HN - N:UNK1:O			2.63993	
	A:ASN317:HD22 - N:UNK1:O			2.08149	
	N:UNK1:H - A:SER236:OG			1.84952	
	N:UNK1:H - A:ASN317:OD1			2.4615	
			A:HIS423 - N:UNK1	5.02906	
			N:UNK1 - A:ILE419	5.19732	
Caffeic acid	A:ASN317:HD22 - N:UNK1:O			2.61486	-7.3
	N:UNK1:H - A:GLU429:O			2.2289	
	N:UNK1:H - A:GLU422:OE1			2.94661	
		A:LYS156:NZ - N:UNK1		4.16194	
			A:PHE314 - N:UNK1	4.7899	
			N:UNK1 - A:ALA418	4.97655	
			N:UNK1 - A:ILE419	5.24291	
GLC	N:UNK1:H - A:ASN235:O			2.81062	-5.9
	N:UNK1:H - A:HIS423:NE2			2.3532	
	N:UNK1:H - A:GLU422:OE1			2.54218	
	A:GLY160:CA - N:UNK1:O			3.32705	
Acarbose (ligand control)	A:SER304:HG - N:UNK1:O			1.98971	-8.0
	N:UNK1:H - A:ASP307:OD2			2.96388	
	N:UNK1:H - N:UNK1:O			2.34045	
	N:UNK1:H - A:GLU411:OE2			2.60896	
	N:UNK1:H - A:GLU411:OE2			2.62251	
	N:UNK1:H - N:UNK1:O			2.17359	
	A:HIS280:CE1 - N:UNK1:O			3.30083	
	A:ARG315:CD - N:UNK1:O			3.1535	
	N:UNK1:C - A:PRO312:O			3.59631	
Miglitol	N:UNK1:H - A:TYR158:O			2.44135	-5.8

Voglibose	N:UNK1:H - A:ASP352:OD2		2.32418	-5.9
	N:UNK1:H - A:GLN353:OE1		2.2137	
	N:UNK1:H - A:LYS156:O		2.40716	
	N:UNK1:H - A:ASP242:OD2		2.75118	
	N:UNK1:H - A:SER311:O		2.49004	
	N:UNK1:H - A:PRO312:O		2.46583	
		N:UNK1:C - A:TYR158	3.72163	

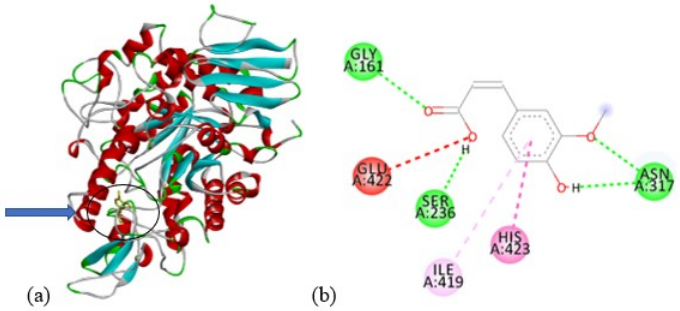

Figure 16. Visualization of 3D and 2D Molecular Interaction (a) and (b) Between α-glucosidase and Ferulic Acid

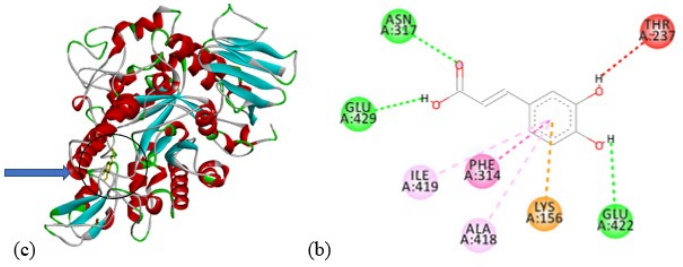

Figure 17. Visualization of 3D and 2D Molecular Interaction (a) and (b) Between α-glucosidase and Caffeic Acid

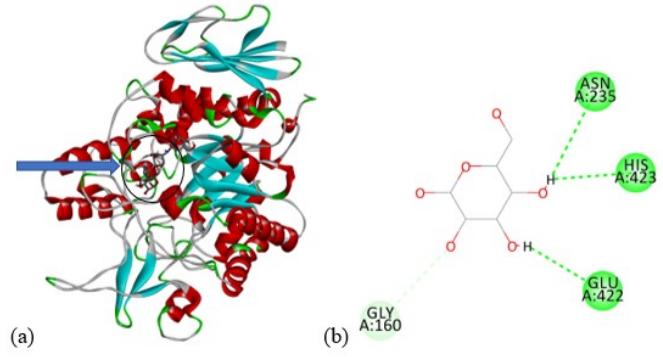

Figure 18. Visualization of 3D and 2D Molecular Interaction (a) and (b) Between α-glucosidase and Acarbose

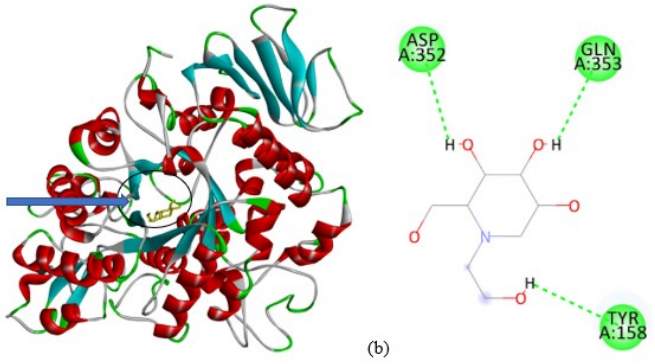

Figure 19. Visualization of 3D and 2D Molecular Interaction (a) and (b) Between α-glucosidase and Miglitol

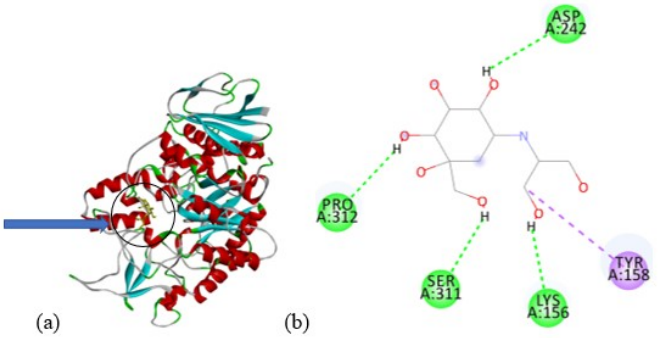

Figure 20. Visualization of 3D and 2D Molecular Interaction (a) and (b) Between α-glucosidase and Voglibose

epicatechin were present in both extracts with retention time. Tables 1 and 2 present the two groups of flavonoids, including flavonols (rutin, quercetin, and isorhamnetin), flavan-3-ols (epicatechin), and one group of cinnamic acids such as caffeic acid and ferulic acid). A prior relevant study reported that *C. tagal* leaves contained several compounds, such as alkaloid, tannin, terpenoid, glycoside, steroid, saponin, flavonoid, coumarin, phenolic, and quinones (Jadhav, 2019). Elaborating further, Wang et al. (2012) reported that the predominant chemical compounds of *Ceriops sp.* genus were terpenoid, especially triterpenoid, as reported in other studies (Canusa et al., 2021; Mahmud et al., 2018;Ramadhan et al., 2020; Jadhav, 2019). In 1971, procyanidin was isolated from *C. roxburghiana* Mahmud et al. (2018). Even though triterpenoid was detected as a

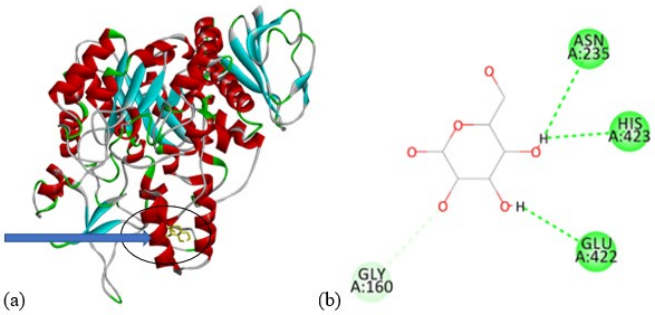

Figure 21. Visualization of 3D and 2D Molecular Interaction (a) and (b) Between α-glucosidase and GLC

prominent compound in *Ceriops sp.*; this study, however, was capable of detecting the six flavonoids from *C. decandra* leaves. Prior studies (Proença et al., 2019; Proença et al., 2022; Şöhretoğlu and Sari, 2020) reported that flavonoid such as rutin, quersetin, epicatechin and isorhamnetin had a potential to inhibit α-glucosidase and α-amylase activities. Therefore, *C. decandra* leaves indicated its potential as an herbal medicine antidiabetic.

3.2 Drug-likeness and Toxicity Analysis

The pharmacological properties of phenolic compounds identified from *C. decandra* leaves were evaluated in accordance with Lipinski's rule. Based on this rule, indicators such as the molecular weights (MW) of < 500 Da, lipophilicity (log P) of < 5, number of hydrogen bond acceptors (HBA) of ≤ 10, and number of hydrogen donors (HBD) of ≤ 5, were applied to assess the drug-likeness of flavonoid from *C. decandra* leaves extract (Lipinski et al., 1997). Among the phenolic compounds identified from *C. decandra* leaves, only rutin did not fulfill the rule because the molecular weight was >500. As presented by Table 3, it is apparent that quercetin, epicatechin, isorhamnetin, caffeic acid, and ferulic acid were in accordance with Lipinski's rule. Therefore, those compounds possess drug-likeness properties, thereby indicating that it could be applied for molecular docking to determine the molecular interaction with the receptor. However, rutin had three violations (MW > 500, HBA ≥10, and HBD ≥5); therefore, it does not possess drug-likeness properties. Only isorhamnetin depicted low gastrointestinal absorption. The phenolic compounds were determined for their toxicity level and class. As shown in Table 3, all of the compounds did not exhibit any toxicity, and the toxicity degree of the compounds was around levels 3-6. In general, the drug-likeness concept has been applied to select compounds with desirable properties of high ADMET (absorption, distribution, metabolism, excretion, and toxicity) profiles (Tian et al., 2015). The phenolic compounds exhibited high gastrointestinal absorption except for isorhamnetin. In particular, toxicity level has been classed into six levels according to the LD_{50} value, which is: class I: $LD_{50} \leq 5$, class II: $5 < LD_{50} \leq 50$, class III: $50 < LD_{50} \leq 300$, class IV: $300 < LD_{50} \leq 2000$, class V: $2000 < LD_{50} \leq 5000$ and class VI: $LD_{50} > 5000$. As illustrated in Table 3, all of the presented compounds did not indicate any toxicity sign because none of the compounds were classified in class I. The presentation also indicated that all phenolic compounds extracted from *C. decandra* leaves were safe for human consumption (Banerjee et al., 2018a; Banerjee et al., 2018b; Drwal et al., 2014; Sadeghi et al., 2021).

3.3 Molecular Interaction Analysis

The result of molecular docking between phenolic compounds extracted from *C. decandra* leaves extract with α-amylase enzyme was provided in Table 4. In this study, acarbose, miglitol, and voglibose as ligands controls were applied to compare the binding energy between ligand control and phenolic compounds. According to the molecular interaction, the binding energy of all compounds was different, varying from -6.5 to -8.7 kcal/mol. As reported in this study, acarbose, miglitol, and voglibose presented different binding energy, which was -8.1, -5.3, and -6.4, respectively. Formerly, acarbose, miglitol, and voglibose were applied as standard drugs to inhibit the activity of both α-glucosidase in the diabetic patient (Bischoff, 1994).

The binding energy of rutin (-8.7 kcal/mol), epicatechin (-8.6 kcal/mol), quercetin (-8.2 kcal/mol), and isorhamnetin (-8.3 kcal/mol) were lower than that of ligand controls, such as in acarbose (-8.1kcal/mol), miglitol (-5.3 kcal/mol) and voglibose (-6.4 kcal/mol). Moreover, the binding energy of the cinnamic acid group, including ferulic acid and caffeic acid, was higher than acarbose. Both ferulic acid and caffeic acid identified from ethyl acetate extract presented similar binding energy with the value of -6.5 kcal/mol, which was lower than the binding energy of miglitol (-5.3 kcal/mol) and voglibose (-6.4 kcal/mol). The highest inhibition towards enzyme activity was shown on the lowest binding energy. Therefore, flavonoids, including: rutin, epicatechin, quercetin, and isorhamnetin, exhibited higher inhibition activity than those in ferulic acid and caffeic acid.

Visualization of molecular interaction between α-amylase and phenolic compounds was depicted in Figure 1-6. Among the flavonoid compounds, the lowest value of binding energy is rutin (-8.7 kcal/mol). Therefore, rutin has the highest inhibitory activity against α-amylase (Adinortey et al., 2022). In this study, rutin has H-bond interaction with amino acid residues such as Arg252, Arg398, Arg421, Gln404, Pro4, Asp290, and Pro332 (Figure 2). Miglitol and voglibose formed H-bonds with amino acid residues Arg398 and Pro332 (Figure 8 and 9). Hence, it can be observed that rutin, miglitol, and voglibose bound to Arg398 and Pro332 and, therefore, rutin inhibited α-amylase by competitive inhibition type. In addition, the amino acid residues such as Arg398 and Pro 332 formed H-bond with miglitol, voglibose, and myricetin (MYC) (Figure 10). It was reported that the structure of 4GQR was complexed with myricetin, thus chosen as a receptor human pancreatic α-amylase (Casacchia et al., 2019).

The binding energy of ferulic acid (-6.5 kcal/mol) was higher compared to the binding energy of other flavonoids.

As a result, ferulic acid indicated the lowest inhibiting activity against α-amylase. Based on the molecular interaction (Figure 6-11), the complexity of ferulic acid with amino acid Ser298 and the complexity of ferulic acid with the amino acids Arg398 and Pro332 had H-bonds interaction. As reported by a prior study Sadeghi et al. (2021), the overlap of ferulic acid with ligand control indicated that common amino acids were involved in the interaction between ferulic acid and ligand control, including acarbose (Ser298) and miglitol and voglibose (Arg398 and Pro332). Therefore, ferulic acid inhibited α-amylase through competitive inhibition.

The complex of quercetin with receptor had hydrogen bond (Glu233), electrostatic interactions (Asp300), and hydrophobic bond (Asp300) (Figure 1). Furthermore, amino acid residues of Glu233, Asp197, and Asp300 are putative active site residues in α-amylase in order to break the starch (Nahoum et al., 2000). The flavonoid compounds such as epicatechin (Figure 3) and isorhamnetin (Figure 4) formed a conventional hydrogen bond (Asp197) and hydrophobic bond (Trp59), indicating that flavonoids bound on α-amylase. In a prior study, amino acid residues which were identified were: Trp58, Trp59, Tyr62, Gln63, and Asp197 bound to flavonoids (Martinez-Gonzalez et al., 2019). The amino acid Asp402 had hydrogen bond interaction with ligand control (voglibose, miglitol, acarbose) and ligand native (myricetin). Hence, the overlap between amino acid residue and ligand control indicated that some common amino acids were involved in the inhibition activity (Sadeghi et al., 2021) through competitive inhibition.

The result of molecular docking analysis between the ligands, including control, phenolic compounds, and native and receptors (PDB ID 3A4A), is provided in Table 5. Based on the binding energy of phenolic compounds, it varies, such as -6.9 kcal/mol (ferulic acid), -7.3 kcal/mol (caffeic acid), -8.4 kcal/mol (epicatechin), -8.4 kcal/mol (isorhamnetin), -8.7 kcal/mol (quercetin) and -10.5 kcal/mol (rutin). There are three commercial drugs that have been used as ligand controls such as acarbose, miglitol, and voglibose. The binding energy of commercial drugs included acarbose (-8 kcal/mol), miglitol (-5.8 kcal/mol), and voglibose (-5.9 kcal/mol). Moreover, the binding energy of ligand native (GLC) was -5.9 kcal/mol. The result further indicated that the binding energy of phenolic compounds such as epicatechin (-8.4 kcal/mol), isorhamnetin (-8.4 kcal/mol), quercetin (-8.7 kcal/mol), and rutin (-10.5 kcal/mol) was lower than both ligand control and ligand native (-5.9 kcal/mol). Lower binding energy value was correlated to stronger binding between ligand and receptor. Thus, phenolic compounds such as epicatechin, isorhamnetin, quercetin, and rutin were able to bind the active site of the α-glucosidase and to inhibit the activity of the enzyme. According to the molecular interactions and the binding energy value as analyzed in this study, rutin had the lowest binding energy and performed the highest inhibitory activity compared to other phenolic compounds extracted in this study.

As presented in Figure 12-21, both hydrogen and hydrophobic bonds interact among ligand control, phenolic compounds, and ligand native. Previous studies reported that some amino acids (GLU411, ARG315, TYR158, ASP352) play a key role in the interaction of the enzyme and inhibitor at the active site of α-glucosidase (PDB ID 3A4A) (Nipun et al., 2020). Both GLU411 and ARG 315 were involved in the interaction between receptors and ligands such as acarbose, isorhamnetin, epicatechin, and rutin. The complex of TYR158 with ligands including voglibose, miglitol, isorhamnetin, and rutin had hydrogen binding interaction. Several residues involved in the binding of rutin to receptor PDB ID 3A4A were GLU411, ARG315, TYR158, ASP352, LYS156, and ASP242, and these findings were in accordance with prior studies (Zeng et al., 2019). In addition, it was assumed that the hydrogen bonds decreased the hydrophilicity, while the hydrophobicity of α-glucosidase increased the stability of the complex. Insertion of a routine into the active site of the receptor inhibits the entrance of the substrate to decrease catalytic activity. Thus, the changing of conformation inhibited α-glucosidase activity (Zeng et al., 2019). Despite rutin, quercetin also had overlapping amino acid residues with ferulic acid (ASN317 and ILE419) and caffeic acid (ASN317, ALA418, and ILE419). However, there were no similarities between amino acid residue present in native ligands and control ligands. The native ligand (GLC) also had overlapping amino acids with amino acid residues of quercetin, including ASN235, HIS423, and GLU422. *Isomaltase S.* cerevisiae contains 589 amino acids, divided into three domains: A (1-113 dan 190-512), domain B (114-189), and domain C (513-589). ASP352 is one of the residue catalytic located in the C-terminal side of the barrel of domain A (Yamamoto et al., 2010). Rutin bounds ASP352 towards α-glucosidase through hydrogen interactions, revealing that the α-glucosidase was incapable of cleaving carbohydrates when its active site was blocked. As a result, it suppressed glucose absorption and decreased blood glucose level (Nipun et al., 2020). Referring to such results, the binding energy of test compounds in rutin was lower than those in both ligand control and ligan native.

4. CONCLUSION

The different polarity solvents significantly affected the phenolic compounds extracted from *C. decandra* leaves, and this study detected that quercetin, rutin, epicatechin, isorhamnetin, caffeic acid, and ferulic acid were found from the extraction of *C. decandra* leaves. Phenolic compounds identified from both ethyl acetate and methanolic extract had high potential pharmacological properties based on Lipinski's rule, SwissADME, and toxicity class. Based on the molecular interactions, it can be concluded that phenolic compounds identified from ethyl acetate extracts such as quercetin and epicatechin; and methanolic extracts namely quercetin, rutin, epicatechin, and isorhamnetin, were more effective for inhibiting the α-amylase and α-glucosidase than from standard drugs such as acarbose, miglitol, and voglibose.

5. ACKNOWLEDGMENT

This study was funded by Lembaga Penelitian dan Pengabdian Masyarakat (Research and Community Services) of Universitas Brawijaya: Hibah Penelitian Pemula Tahun 2022 (No. 974.32/UN10.C10/PN/2022).

REFERENCES

Adinortey, C. A., G. B. Kwarko, R. Koranteng, D. Boison, I. Obuaba, M. D. Wilson, and S. K. Kwofie (2022). Molecular Structure-based Screening of the Constituents of Calotropis Procera Identifies Potential Inhibitors of Diabetes Mellitus Target Alpha Glucosidase. *Current Issues in Molecular Biology*, **44**(2); 963–987

Alamsjah, M. A. and M. FauzulImron (2021). Monitoring of Diversity, Characteristics, Threatening Rate and Potency of Mangrove Vegetation in Denpasar, Bali, Indonesia. *Plant Archives*, **21**(1); 592–599

Askama, S., S. Wahyuni, and M. Mashuni (2017). Pengaruh Penambahan Bubuk Daun Tanaman Mangrove (Ceriops sp.) Terhadap Karakteristik Organoleptik Produk Cokelat Batang (Effect of The Addition of Mangrove Plant (Ceriops sp.) Leaf on The Organoleptic Characteristics of Chocolate Bars). *Jurnal Sains Dan Teknologi Pangan*, **2**(4); 729–735 (in Indonesia)

Banerjee, P., F. O. Dehnbostel, and R. Preissner (2018a). Prediction is a Balancing act: Importance of Sampling Methods to Balance Sensitivity and Specificity of Predictive Models Based on Imbalanced Chemical Data Sets. *Frontiers in Chemistry*, **1**(11); 1–11

Banerjee, P., A. O. Eckert, A. K. Schrey, and R. Preissner (2018b). ProTox-II: a Webserver for the Prediction of Toxicity of Chemicals. *Nucleic Acids Research*, **46**(W1); 257–263

Bibi, S. N., M. M. Fawzi, Z. Gokhan, J. Rajesh, N. Nadeem, R. K. RR, A. RDDG, and S. K. Pandian (2019). Ethnopharmacology, Phytochemistry, and Global Distribution Of Mangroves-a Comprehensive Review. *Marine Drugs*, **17**(4); 1–82

Bischoff, H. (1994). Pharmacology of Alpha-glucosidase Inhibition. *European Journal of Clinical Investigation*, **24**; 3–10

Canusa, B. S., I. L. Lawag, O. B. Villaflores, V. D. Wagh, M. Korinek, Y.-H. Tsai, F.-R. Chang, and A. M. Aguinaldo (2021). α-Glucosidase Inhibitors from the Bark Extract of Ethno-Antidiabetic Ceriops tagal (Perr.) CB Rob. *Philippine Journal of Science*, **151**(S1); 25–60

Casacchia, T., M. A. Occhiuzzi, F. Grande, B. Rizzuti, M. C. Granieri, C. Rocca, A. Gattuso, A. Garofalo, T. Angelone, and G. Statti (2019). A Pilot Study on the Nutraceutical Properties of the Citrus hybrid Tacle® as a Dietary Source of Polyphenols for Supplementation in Metabolic Disorders. *Journal of Functional Foods*, **52**; 370–381

Chen, L. and Y. H. Kang (2013). In Vitro Inhibitory Effect of Oriental Melon (Cucumis melo L. Var. Makuwa Makino) Seed on Key Enzyme Linked to Type 2 Diabetes: Assessment of Anti-diabetic Potential of Functional Food. *Journal of Functional Foods*, **5**(2); 981–986

Derosa, G. and P. Maffioli (2012). α-Glucosidase Inhibitors and Their Use in Clinical Practice. *Archives of Medical Science: AMS*, **8**(5); 899–906

Dham, S. V. H. S. . B. M. A., S. (2006). The Role of Complementary and Alternative Medicine In Regenerative Medicine. *Current Diabetes Reports*, **6**(3); 251–258

Drwal, M. N., P. Banerjee, M. Dunkel, M. R. Wettig, and R. Preissner (2014). ProTox: a Web Server for the in Silico Prediction of Rodent Oral Toxicity. *Nucleic Acids Research*, **42**(W1); 53–58

Hardoko, H., Y. E. Puspitasari, and E. Suprayitno (2015). -Glucosidase Inhibitory Activities of Rhizophora Mucronata Fruitpowder. *International Journal of ChemTech Research*, **8**(1); 211–215

Hardoko, H., B. B. Sasmito, and Y. E. Puspitasari (2016). Antidiabetic and Antioxidant Activities of Tannin Extract of Rhizophora Mucronata Leaves. *Journal of Chemical and Pharmaceutical Research*, **8**(3); 143–148

Hardoko, H., B. B. Sasmito, and Y. E. Puspitasari (2017). Tannin Extract Characterization of Young Mangrove Rhizophora Mucronata Leaves as Ingredients for Diabetic Functional Food. *Asian Journal of Microbiology, Biotechnology and Environmental Sciences*, **19**(2); 331–336

Jadhav, B. (2019). Phytochemical Composition, In Vitro Studies On A-Amylase And A-Glucosidase Inhibitory Activity Of Selected Mangrove Plants. *International Journal of Pharmaceutical Sciences and Drug Research*, **11**(5); 181–186

Kharroubi, A. T. and H. M. Darwish (2015). Diabetes Mellitus: The Epidemic of the Century. *World Journal of Diabetes*, **6**(6); 850–867

Kim, Y., J. B. Keogh, and P. M. Clifton (2016). Polyphenols and Glycemic Control. *Nutrients*, **8**(1); 1–27

Lauritano, C. and A. Ianora (2016). Marine Organisms with Anti-diabetes Properties. *Marine Drugs*, **14**(12); 1–14

Lawag, I. L., A. M. Aguinaldo, S. Naheed, and M. Mosihuzzaman (2012). α-Glucosidase Inhibitory Activity of Selected Philippine Plants. *Journal of Ethnopharmacology*, **144**(1); 217–219

Lipinski, C. A., F. Lombardo, B. W. Dominy, and P. J. Feeney (1997). Experimental and Computational Approaches to Estimate Solubility and Permeability in Drug Discovery and Development Settings. *Advanced Drug Delivery Reviews*, **23**(1-3); 3–25

Mahmud, I., N. Shahria, S. Yeasmin, A. Iqbal, E. H. Mukul, S. Gain, J. A. Shilpi, and M. K. Islam (2018). Ethnomedicinal, Phytochemical and Pharmacological Profile of A Mangrove Plant Ceriops Decandra Griffdin Hou. *Journal of Complementary and Integrative Medicine*, **16**(1); 20170129

Mahmud, M. (2011). Vegetasi Mangrove Sebagai Bahan Makanan Pada Empat Suku Di Papua Mangrove Vegetation as Foods Amongst Ethnics in Papua. *Biota: Jurnal Ilmiah Ilmu-Ilmu Hayati*, **16**(1); 88–94 (in Indonesia)

Martinez-Gonzalez, A. I., Á. Díaz-Sánchez, L. De La Rosa,

I. Bustos Jaimes, and E. Alvarez Parrilla (2019). Inhibition of α-amylase by Flavonoids: Structure Activity Relationship (SAR). *Spectrochimica Acta Part A: Molecular and Biomolecular Spectroscopy*, **206**; 437–447

Nahoum, V., G. Roux, V. Anton, P. RougÉ, A. Puigserver, H. Bischoff, B. Henrissat, and F. Payan (2000). Crystal Structures of Human Pancreatic α-amylase in Complex with Carbohydrate and Proteinaceous Inhibitors. *Biochemical Journal*, **346**(1); 201–208

Nipun, T. S., A. Khatib, Z. Ibrahim, Q. U. Ahmed, I. E. Redzwan, M. Z. Saiman, F. Supandi, R. Primaharinastiti, and H. R. El Seedi (2020). Characterization of α-glucosidase Inhibitors from Psychotria Malayana Jack Leaves Extract Using LC-MS-based Multivariate Data Analysis and in-silico Molecular Docking. *Molecules*, **25**(24); 5885

Prabowo, R. E. (2018). Peluang Bisnis Kuliner Buah Mangrove (Culinary Business Opportunities of Mangrove Fruit). *Prosiding Seminar Nasional Multidisiplin Ilmu*, **7**; 978–979 (in Indonesia)

Proença, C., M. Freitas, D. Ribeiro, S. M. Tomé, E. F. Oliveira, M. F. Viegas, A. N. Araújo, M. J. Ramos, A. M. Silva, P. A. Fernandes, et al. (2019). Evaluation of A Flavonoids Library for Inhibition of Pancreatic α-amylase Towards A Structure–activity Relationship. *Journal of Enzyme Inhibition and Medicinal Chemistry*, **34**(1); 577–588

Proença, C., D. Ribeiro, M. Freitas, and E. Fernandes (2022). Flavonoids as Potential Agents in the Management of Type 2 Diabetes Through the Modulation of α-amylase and α-glucosidase Activity: A Review. *Critical Reviews in Food Science and Nutrition*, **62**(12); 3137–3207

Ramadhan, R., P. Phuwapraisirisan, I. Kusuma, and R. Amirta (2020). Ethnopharmacological Evaluation of Selected East Kalimantan Flora For Diabetes Therapy: The Isolation of Lupane Triterpenoids as α-glucosidase Inhibitors From Ceriops Tagal (perr) (PERR) C.B.ROBB. *Rasayan Journal of Chemistry*, **13**(3); 1727–1734

Riyaphan, J., D. C. Pham, M. K. Leong, and C. F. Weng (2021). In Silico Approaches to Identify Polyphenol Compounds As α-glucosidase and α-amylase Inhibitors Against Type-II Diabetes. *Biomolecules*, **11**(12); 1877

Sadeghi, M., M. Moradi, H. Madanchi, and B. Johari (2021). In Silico Study of Garlic (Allium sativum L.) Derived Compounds Molecular Interactions with α-glucosidase. *In Silico Pharmacology*, **9**; 1–8

Sivakumar, K., S. Kannappan, B. Vijayakumar, K. P. Jithendran, S. Balasubramaniam, and A. Panigrahi (2021). Molecular Docking Study of Bio-inhibitors Extracted From Marine Macro-alga Ulva Fasciata Against Hemolysin Protein of Luminescence Disease-causing Vibrio Harveyi. *Archives of Microbiology*, **203**(7); 4243–4258

Şöhretoğlu, D. and S. Sari (2020). Flavonoids as Alpha-glucosidase Inhibitors: Mechanistic Approaches Merged with Enzyme Kinetics and Molecular Modelling. *Phytochemistry Reviews*, **19**(5); 1081–1092

Tian, S., J. Wang, Y. Li, D. Li, L. Xu, and T. Hou (2015). The Application of in Silico Drug-likeness Predictions in Pharmaceutical Research. *Advanced Drug Delivery Reviews*, **86**; 2–10

Trinh, B. T., D. Staerk, and A. K. Jäger (2016). Screening for Potential α-glucosidase and α-amylase Inhibitory Constituents from Selected Vietnamese Plants Used to Treat Type 2 Diabetes. *Journal of Ethnopharmacology*, **186**; 189–195

Trott, O. and A. J. Olson (2010). AutoDock Vina: Improving the Speed and Accuracy of Docking with A New Scoring Function, Efficient Optimization, and Multithreading. *Journal of Computational Chemistry*, **31**(2); 455–461

Udrea, A. M., G. G. Pircalabioru, A. A. Boboc, C. Mares, A. Dinache, M. Mernea, and S. Avram (2021). Advanced Bioinformatics Tools in the Pharmacokinetic Profiles of Natural and Synthetic Compounds with Anti-diabetic Activity. *Biomolecules*, **11**(11); 1692

Yamamoto, K., H. Miyake, M. Kusunoki, and S. Osaki (2010). Crystal Structures of Isomaltase From Saccharomyces Cerevisiae and in Complex with its Competitive Inhibitor Maltose. *The FEBS journal*, **277**(20); 4205–4214

Zeng, L., H. Ding, X. Hu, G. Zhang, and D. Gong (2019). Galangin Inhibits α-glucosidase Activity and Formation of Non-enzymatic Glycation Products. *Food Chemistry*, **271**; 70–79

Zhang, B. W., X. Li, W. L. Sun, Y. Xing, Z. L. Xiu, C. L. Zhuang, and Y. S. Dong (2017). Dietary Flavonoids and Acarbose Synergistically Inhibit α-glucosidaseand Lower Postprandial Blood Glucose. *Journal of Agricultural and Food Chemistry*, **65**(38); 8319–8330

